Solvent Effect on Mineral Modification: Selective Synthesis of Cerium Compounds by a Facile Solution Route

Shaofeng Chen,[a, b] Shu-Hong Yu,*[a, b] Bo Yu,[b] Lei Ren,[c] Weitang Yao,[b] and Helmut Cölfen[d]

Abstract: A mild solution method has been designed for the selective synthesis of orthorhombic and hexagonal $CeOHCO_3$, as well as cubic CeO_2 crystals in an ethanol/water mixed solvent. This study added a new example for selectively controlling different cerium compounds by manipulating the balance between kinetics and thermodynamics in a mixed solvent system. The competitive reactions taking place in the ethanol/water system, phase transition, and shape evolution were fully investigated: they were found to be strongly dependent on the composition of the reaction media. The influence of the ethanol content in the mixed solvent and that of the reaction time on the phase transition and shape of orthorhombic and hexagonal $CeOHCO_3$ crystals is discussed in detail. Metastable hexagonal $CeOHCO_3$ can be trapped, even at 80 °C, in the ethanol/water solvent mixture without the need for the high temperature adopted by previous hydrothermal approaches. The evolution process of orthorhombic and metastable hexagonal phases under mild solution conditions is discussed for the first time. Supersaturation will become faster and more evident when water is replaced by ethanol, because the inorganic salts have a lower solubility in ethanol than in water, and this will generally favor the formation of the kinetic phase, such as the hexagonal $CeOHCO_3$ phase reported in this paper. The optical properties of the products with different phases and composition were investigated.

Keywords: cerium · crystal growth · hydroxycarbonate · luminescence · metastable phases · phase transitions

Introduction

Rare-earth compounds have been extensively utilized as functional materials,[1–5] because of their electronic properties as well as their optical and chemical characteristics that arise from their 4f electrons. Most of their properties are dependent on the composition, crystal type, shape, and size. Among compounds of the rare-earth family, Pr, Tb, and Ce, in particular, have attracted a lot of attention on account of their special bonding states of atoms or ions,[1,2,6,7] as well as their wide range of applications in catalysis,[8–10] luminescent devices,[11,12] superconductivity,[13,14] and other areas.[15–17] Inorganic salts of cerium,[18–20] which have easily controllable ligand environments, are popular in preparing compositions containing cerium. For this reason, cerium hydroxycarbonate was synthesized,[20–24] and the selection of shape and crystal polymorphs was further investigated. Recently, a hydrothermal process has been employed for the synthesis of cerium hydroxycarbonate. The temperature was found to be a key parameter for the phase transition from orthorhombic $CeOHCO_3$ to a hexagonal phase.[24] Wang et al.[20] reported that the quantity of urea in the $Ce(NO_3)_3$/urea reaction system can evidently change the shape of orthorhombic $CeOHCO_3$. In addition, the presence of polyvinylpyrrolidone (PVP) is helpful to form orthorhombic $CeOHCO_3$ at a relatively low temperature.[23]

Manipulation of the thermodynamic and kinetic control processes plays a key role in crystal growth, which determines the final crystal habit, phase, shape, and structure.[25,26]

[a] S. Chen, Prof. Dr. S.-H. Yu
Hefei National Laboratory for Physical Sciences at Microscale
University of Science and Technology of China
Hefei 230026 (P. R. China)
Fax: (+86) 551-3603040
E-mail: shyu@ustc.edu.cn

[b] S. Chen, Prof. Dr. S.-H. Yu, B. Yu, W. Yao
Department of Materials Science and Engineering
University of Science and Technology of China
Hefei 230026 (P. R. China)
Fax: (+86) 551-3603040

[c] Dr. L. Ren
Biomedical Engineering Research Center
Xiamen University
Xiamen 361005 (P.R. China)

[d] Dr. H. Cölfen
Department of Colloid Chemistry
Max Planck Institute of Colloids and Interfaces
MPI Research Campus Golm, 14424 Potsdam (Germany)

Supporting information for this article is available on the WWW under http://www.chemeurj.org or from the author.

DOI: 10.1002/chem.200306066

The examples of fine control over the thermodynamic/kinetic balance of the formation of biominerals with complex forms and specific polymorphs can be found in the bodies or shells of various organisms. In general, kinetic control is based predominantly on modification of the activation-energy barriers of nucleation, growth, and phase transformation, for which usually either a constrained reaction environment, such as a polymer matrix[27] was used or the formation of amorphous particles often preceded the complex structure development under control of molecular templates.[25]

Solvent effects on the shape, size, and phase formation for various semiconductor nanocrystals under solvothermal conditions have been reported previously.[28] Only a few examples dealing with phase transitions of semiconductor nanocrystals at high pressures[29] have been reported, including the solvent-induced phase transition of ZnS nanocrystallites with a size of 3 nm from the hexagonal to the cubic phase at ambient temperature and pressure.[30] Several previous investigations have been reported on the use of simple alcohols in controlled calcium carbonate crystal growth.[26,31–34] The results mainly show that crystallization of $CaCO_3$ crystals under ambient conditions in the presence of different alcohol media has shown remarkable effects on the stabilization of the vaterite phase and an accelerated crystal growth rate. Recently, we demonstrated that metastable hexagonal In_2O_3 nanofibers can be templated under ambient pressure by annealing InOOH nanofibers that had been obtained from a solvothermal reaction in ether.[35]

Herein, we present a mild solution-based route to selectively synthesize orthorhombic and hexagonal $CeOHCO_3$, as well as cubic CeO_2 nanocrystals in an ethanol/water solvent mixture. The competitive reactions in the ethanol/water system, the phase transition, and shape evolution were fully investigated. They were found to be strongly dependent on the composition of the ethanol/water medium. The influence of the ethanol content in the mixed solvent and the reaction time on the stabilization of the hexagonal phase is discussed in detail. The optical properties of the products with different phases and compositions were investigated.

Experimental Section

All chemicals used in this study are commercially available (Aldrich) and were used without further purification. In a typical synthesis $Ce(NO_3)_3{\cdot}6H_2O$ (0.434 g, AR purity: 99%) and urea (0.36 g, CR purity: 99.0%) were added to a solvent mixture of distilled water and anhydrous ethanol (total amount: 20 mL) under vigorous magnetic stirring. The clear solution was poured into a 20 mL wide-mouthed jar that was then closed and kept at 80°C for one day. The solution was then air-cooled to room temperature. The resulting products were centrifuged, washed with distilled water, and dried at 60°C. The hydrothermal reaction was carried out in a Teflon-lined autoclave, as described previously.

The obtained sample was characterized on a (Philips X'Pert Pro Super) X-ray powder diffractometer with $Cu_{K\alpha}$ radiation ($\lambda = 1.541874$ Å). The size and morphology were determined with a JEOL JSM-6700F scanning electron microscope (SEM). Photoluminescence (PL) emission was performed at room temperature with a Perkin–Elmer LS55 luminescence spectrometer.

Results and Discussion

Selective synthesis of the cerium compounds: The reaction in pure water at 80°C leads to the formation of pure orthorhombic $CeOHCO_3$ (JCPDS Card 41–13, $a = 5.015$, $b = 8.565$, $c = 7.337$ Å, symmetry group *Pmcn*), as detected by the XRD pattern shown in Figure 1a.

The results obtained in solutions with differing ethanol/water ratios are summarized in Figure 1 and Table 1. This ratio has a significant effect on the phase formation. From the XRD pattern (Figure 1) and Table 1, it can be seen that

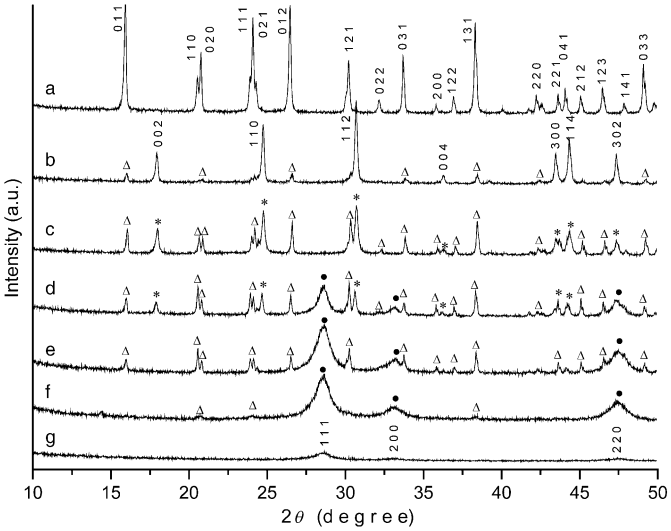

Figure 1. XRD patterns of cerium compositions synthesized at 80°C for 24 h. a) Pure orthorhombic $CeOHCO_3$ (sample 1, pure water). b) Almost pure hexagonal $CeOHCO_3$ (Sample 2, $R = 3$). c) A mixture of almost two nearly identical amounts of orthorhombic and hexagonal $CeOHCO_3$ (Sample 3, $R = 1$). d) A mixture of cubic CeO_2, as well as hexagonal and orthorhombic $CeOHCO_3$ (sample 4, $R = 1/3$). e) A mixture of pure cubic CeO_2 and orthorhombic $CeOHCO_3$ (sample 5, $R = 3/17$). f) A mixture of almost pure cubic CeO_2 containing a minor amount of orthorhombic $CeOHCO_3$ (sample 6, $R = 1/9$). g) Pure cubic CeO_2 (Sample 7, pure alcohol). Solvent composition: total volume is 20 mL, R = volume of distilled water:volume of anhydrous ethanol (v/v). △ orthorhombic $CeOHCO_3$ (JCPDS file no. 41–13), ∗ hexagonal $CeOHCO_3$ (JCPDS file no. 32–189), ● cubic CeO_2 (JCPDS file no. 75–390).

Table 1. The summary of the main results on the products obtained under different solvent conditions but otherwise unaltered experimental conditions.

Sample no.	Composition of solvents		Products detected by XRD
	Distilled water [mL]	Ethanol [mL]	
1	20	–	orthorhombic $CeOHCO_3$
2	15	5	hexagonal $CeOHCO_3$,[a] orthorhombic $CeOHCO_3$[b]
3	10	10	orthorhombic and hexagonal $CeOHCO_3$
4	5	15	cubic CeO_2, orthorhombic, hexagonal $CeOHCO_3$
5	3	17	cubic CeO_2,[a] orthorhombic $CeOHCO_3$[b]
6	2	18	cubic CeO_2,[a] orthorhombic $CeOHCO_3$[b]
7	–	20	cubic CeO_2

[a] Dominant phase. [b] Minor amount in the product.

if the amount of anhydrous ethanol is increased to 5 mL, the hexagonal phase $CeOHCO_3$ appeared in the product (JCPDS Card 32–189, $a=7.238$, $c=9.959$ Å), indicating that this phase could be formed as a result of a change in the local solution conditions, such as alcohol content and pH value. In contrast, a previous study showed that the hexagonal phase can only appear at 180 °C under autogenous pressure in pure water through a hydrothermal process.[24] However, the present result suggests that the presence of ethanol is very favorable for the formation and stabilization of the hexagonal phase, even at temperatures as low as 80 °C under ambient pressure. It is well-known that physicochemical solvent properties, such as polarity, viscosity, and softness, will strongly influence the solubility and transport behavior of the precursors.[36] In the present system, the addition of ethanol changes the chemical properties of the solvent, such as dielectric constant, interionic attraction, and the solute–solvent interaction as a result of the solubility difference,[33] as well as the pH value of the local solution, which could have significant effect on the crystal growth and phase formation in the present case. In addition, the appearance of the metastable hexagonal phase under the mild conditions employed could be understandable from the viewpoint of thermodynamics/kinetics: a change in the solution properties will either minimize the free-energy difference between the orthorhombic and hexagonal phase or change the pH value of the solution under the same conditions, which will favor the formation of the metastable hexagonal phase. This phenomenon is quite similar to the more favorable formation of vaterite than calcite under more acidic conditions.[37] In addition, the internal energy difference between the hexagonal and orthorhombic phases could be very small under certain experimental conditions. Also, supersaturation will become faster and more evident by replacing water with ethanol, because the inorganic salts have a lower solubility in ethanol than in water; this will generally favor the formation of the kinetic phase, such as hexagonal $CeOHCO_3$ phase in the present case.

As the volume of ethanol increases from 5 to 10 mL, the relative intensity of the orthorhombic $CeOHCO_3$ phase increases, as shown in Figure 1b and c. In addition, a cubic CeO_2 phase appears when the amount of ethanol reaches 15 mL. This phase coexists with the hexagonal and orthorhombic $CeOHCO_3$ phases (Figure 1d). When the amount of ethanol was increased to 17–18 mL, the formation of hexagonal $CeOHCO_3$ phase was suppressed (Figure 1e and f). Pure CeO_2 nanoparticles were obtained when the reaction was performed in pure ethanol (20 mL) (Figure 1g).

Shape and phase evolution in the ethanol/water system: The shape evolution was investigated in detail by scanning electron microscopy (SEM). Figure 1a shows that the 011, 012, 020, and 121 diffraction peaks for the pure orthorhombic $CeOHCO_3$ phase are unusually strong compared with to those reported (JCPDS Card 41–13). This indicates that they will be the most exposed faces. In addition, the diffraction intensity of the planes that are parallel to the [100] axis are intensified. The intensity of the (200) peak is very weak compared to that of the (020) peak, implying that the long axis of the particles is the *a* axis. This assumption fits the results observed from SEM quite well (see also the Supporting Information, Figure 1). The SEM image in Figure 2a shows

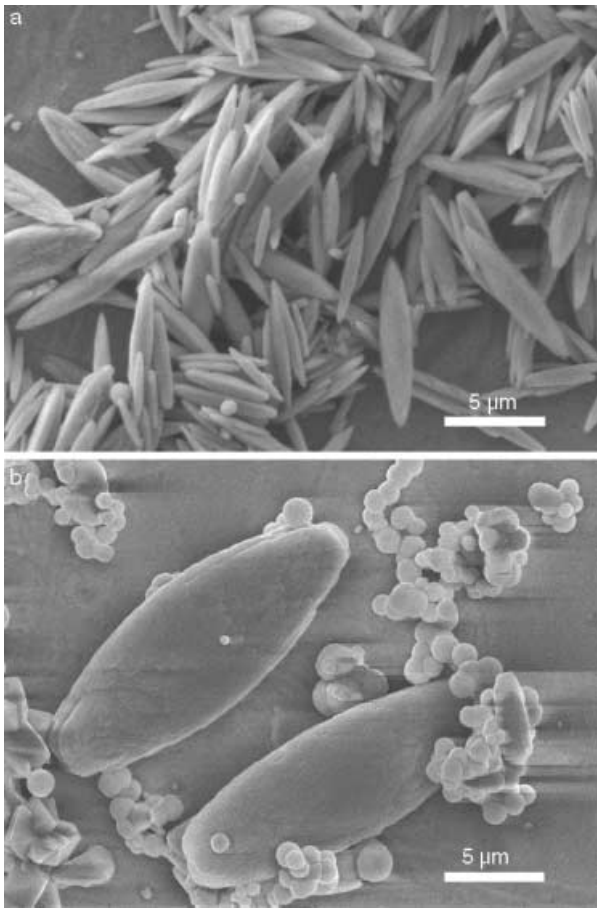

Figure 2. SEM images of the products obtained in the presence of different volumes of ethanol (80 °C, 1 day). a) Orthorhombic $CeOHCO_3$ (solvent: pure water, 20 mL). b) Dominant hexagonal $CeOHCO_3$, coexisting with a minor amount of orthorhombic $CeOHCO_3$ (solvent: 5 mL ethanol + 15 mL water).

that pure orthorhombic $CeOHCO_3$ crystals have a typical sharp, elongated, oval-like morphology with an aspect ratio of ≈ 4, which is similar to that obtained under hydrothermal conditions.[20,24] When 5 mL ethanol was added under identical conditions, spheres of the hexagonal phase with a size of ≈ 200–800 nm were found to be the major product. They coexisted with a minor amount of large orthorhombic $CeOHCO_3$ crystals, as shown in Figure 2b and Figure 3a. The surface of some oval-like crystals in Figure 2b became rougher than that shown in Figure 2a. In addition, the two ends of the oval-like crystals become less sharp and their aspect ratio decreased. A typical high-resolution SEM image in Figure 3b shows that many spherical crystals with round cavities coexisted with incomplete oval-like orthorhombic $CeOHCO_3$ crystals. This could be attributable to the more favorable pH conditions for the formation of hexagonal phase in this reaction stage.

It has been reported that orthorhombic $CeOHCO_3$ is stable even at 160 °C in a hydrothermal system;[24] however,

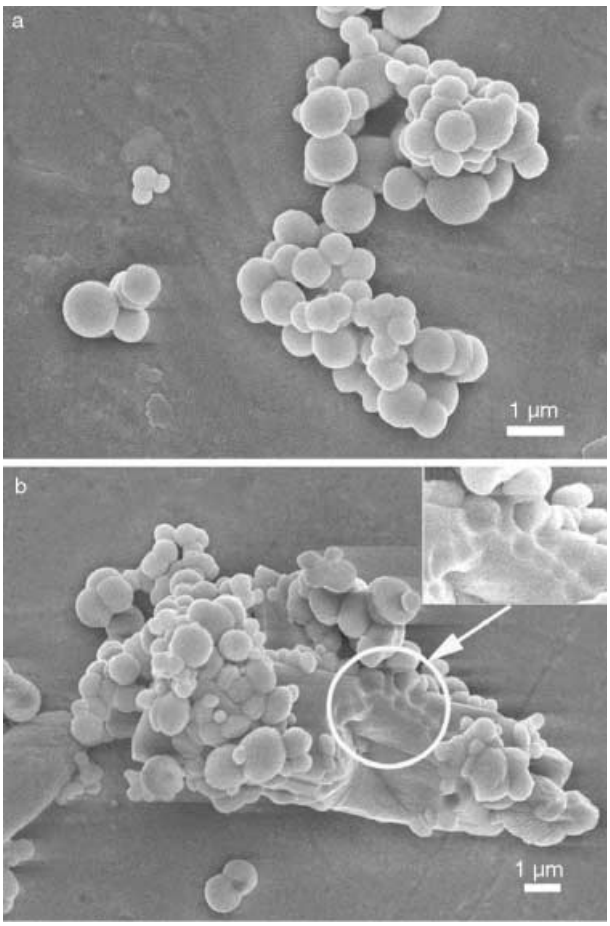

Figure 3. SEM images of the sample obtained in the presence of 5 mL ethanol ($R = 1/3$, ethanol/water, v/v; 80 °C, 1 day). a) Spherical crystals of hexagonal $CeOHCO_3$. b) A typical picture showing the transition process from orthorhombic $CeOHCO_3$ to hexagonal $CeOHCO_3$. Inset: Cavites on the surface of large shuttle-like crystals that were left by spherical hexagonal $CeOHCO_3$ particles.

in our experiments, hexagonal crystal growth often appeared in a mixed ethanol/water solution. The presence of ethanol instead of water will evidently change the local solution conditions for the crystal growth, such as the pH value, which could favor the formation of hexagonal $CeOHCO_3$ phase, similar to the previously reported favored formation of the vaterite phase instead of the calcite phase under more acidic conditions.[37] In addition, the mixed solvent system could also minimize the difference in the phase-transition free energy between the orthorhombic phase and the hexagonal phase; this is similar to that of the transformation from hexagonal ZnS to cubic ZnS.[30] These effects can contribute to the formation of the kinetic phase, and a possible phase transformation can occur even at lower temperatures and ambient pressure. However, the presence of the orthorhombic phase indicates that the altered solvent conditions do not allow for an exclusive polymorph selection. In the inset of Figure 3b inset, spherical cavities can be recognized that appear to originate from spherical hexagonal particles, which are also found on the orthorhombic particle surface. The spherical particles could have dissolved, similar to the sacrificial $CaCO_3$ vaterite dissolution to form hollow calcite spheres,[38] indicating that the hexagonal phase is only metastable relative to the orthorhombic phase.

The presence of abundant ethanol could also reduce the hydration energy and thus the redox potential of Ce^{3+} to make it more easily oxidizable in the presence of a minor amount of O_2, so that a CeO_2 phase can form (see Table 1 and Figure 1). In fact, the reactions are competitive. They are very dependent on the solution composition and local solution chemistry. The main reactions in the system can be expressed as follows [Eqs. (1)–(5)]:

$$CO(NH_2)_2 + H_2O \rightleftharpoons CO_2 + 2\,NH_3 \quad (1)$$

$$CO_2 + H_2O \rightleftharpoons CO_3^{2-} + 2\,H^+ \quad (2)$$

$$NH_3 + H_2O \rightleftharpoons NH_4^+ + OH^- \quad (3)$$

$$Ce^{3+} + OH^- + CO_3^{2-} \rightleftharpoons CeOHCO_3 \quad (4)$$

$$Ce(H_2O)_x(OH^-)_y^{(4-y)+} + H_2O \rightleftharpoons CeO_2 \cdot n\,H_2O + H_3O^+ \quad (5)$$

At 80 °C, urea decomposes, as shown in Equation (1). The resulting gases dissolve in the mixed solvent to yield OH^- and CO_3^{2-}, which are critical for continuation of Equation (4). According to the Gibbs free-energy theory, the calculated Gibbs free energies of Equations (2) and (3) are $-210.16\ kJ\,mol^{-1}$ and $95.31\ kJ\,mol^{-1}$, respectively; this implies that the reaction in Equation (2) occurred more easily. In the present experiment, if 0.36 g urea completely decomposed, as described in Equation (1), it will produce 0.1344 L of CO_2 (under standard conditions) and 0.2688 L of NH_3. Considering their solubility, all produced gases should completely dissolve in water at room temperature. Furthermore, it should be pointed out that the strong hydrogen bonds between the urea and water/ethanol, and the mild reaction temperature (80 °C) could make decomposition rate of urea rather low. This is supported by the fact that the experimental yield of the final product was much lower than the calculated value.

The complete replacement of water by ethanol will suppress the reactions shown in Equations (1)–(3) on account of the poor solubility of CO_2 and NH_3 in ethanol. This results in nonhydrated species in the solution. Therefore, the Ce^{3+} ions are more easily oxidized, even in the presence of a minor amount of O_2. When water is added, the tendency to form $CeOHCO_3$ increases, because CO_2 and NH_3 dissolve more easily in water and will shift Equilibrium (4) towards the right-hand side. The extremely low yield of CeO_2 nanoparticles confirmed this fact.

Under comparable conditions, the solubility of NH_3 in H_2O (700 volume units of NH_3 can dissolve in one volume unit of water under standard conditions) is higher than that of CO_2 (0.385 g per 100 mL water at 273 K under standard pressure) and the concentration of OH^- in the mixed solvent is higher than that of CO_3^{2-}. This is confirmed by the fact that the solvent pH always increased with increasing reaction time. On the basis of the HSAB (hard/soft acid/base) theory, CO_3^{2-} and OH^- are hard bases, and Ce^{3+} is a hard acid. Considering their polarity, ion charge, and ion radius, it is not difficult to bond each other to form $CeOHCO_3$ if the

amount of ethanol is not too high (for example, 5 mL and 10 mL). However, when the amount of ethanol in the system reached the critical value, for example, 15–20 mL, the tendency of Ce^{3+} to oxidize should be considered, because the reactions that rely on a suitable amount of water for the hydration reactions in this system decreased. The results show that the oxidation tendency of Ce^{3+} increased with decreasing amount of water, as clearly confirmed by a series of experimental results shown in Figure 1d–g and Table 1. The coexistence of the three phases with comparable amount of phase composition was found in the presence of 5 mL ethanol (Figure 1d). All diffraction intensities for the {1*kl*} were enhanced relative to those observed in the presence of a smaller amount of ethanol (Figure 1a and c). SEM images in Figure 4 indicated that the orthorhombic crystals tend to become shorter along the *a* axis, and the crystal faces become more exposed and well-developed. When the amount of water present in the system decreases, the reactions in Equations (1)–(3) will be seriously suppressed, and the oxidization of the hydrated precursor $Ce(H_2O)_x(OH^-)_y^{(4-y)+}$ is favored,[39] leading to the formation of CeO_2 nanoparticles. The water-dependent phase formation and transformation was clearly demonstrated in Figure 1d–g and Table 1.

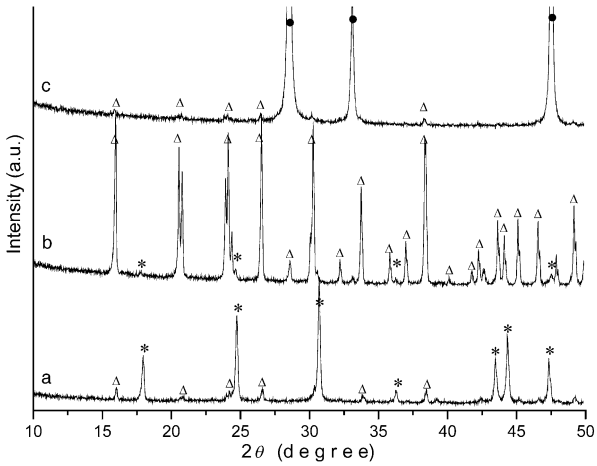

Figure 5. XRD patterns of cerium compounds. a) Almost pure hexagonal $CeOHCO_3$, synthesized in 15 mL distilled water + 5 mL ethanol at 80 °C for 12 h (Sample 2 in Table 1). b) Almost pure orthorhombic $CeOHCO_3$ and a trace amount of hexagonal $CeOHCO_3$, synthesized at 200 °C for 24 h with the same solution composition as that of sample 2. c) A trace amount of orthorhombic $CeOHCO_3$ and almost pure cubic CeO_2, synthesized by hydrothermal treatment of sample 2 powder at 200 °C for 24 h. △ orthorhombic $CeOHCO_3$ (JCPDS file no. 41–13), ∗ hexagonal $CeOHCO_3$ (JCPDS file no. 32–189), ● cubic CeO_2 (JCPDS file no. 75–390).

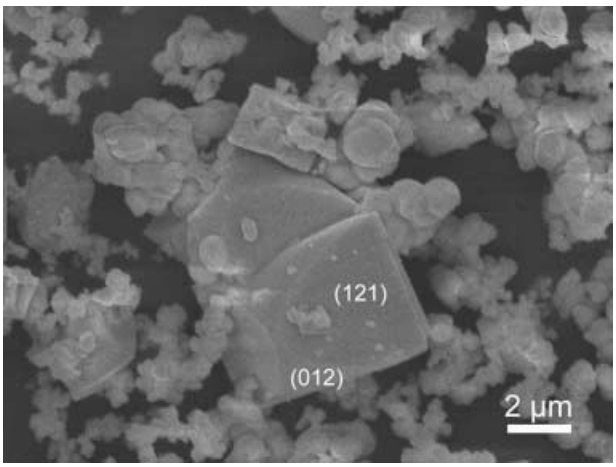

Figure 4. SEM image of a mixture of orthorhombic $CeOHCO_3$, hexagonal $CeOHCO_3$, and CeO_2 nanoparticles synthesized at 80 °C for 24 h (sample 4, ethanol/water, v/v, $R = 1/3$).

Phase stability of $CeOHCO_3$: To distinguish which of the two phases of $CeOHCO_3$ is more stable in the adopted solvent system or at different temperatures, designed experiments were conducted by varying the temperature and hydrothermal treatment of the prepared sample. The solution of precursors in the mixed solvent for the synthesis of sample 2 listed in Table 1 was subjected to hydrothermal treatment in a Teflon-lined autoclave at 200 °C for 24 h. The XRD patterns in Figure 5a and b clearly indicate that orthorhombic $CeOHCO_3$ becomes a dominant phase in the product and only traces of hexagonal $CeOHCO_3$ were detected when the reaction temperature was raised from 80 to 200 °C. As previous results[24] indicate the formation of the hexagonal phase at 180 °C after 12 h, our results indicate a complete transformation of the hexagonal into the orthorhombic phase, probably by a dissolution–recrystallization process, in agreement with the formation of the spherical cavities in Figure 3b.

In order to further understand the phase transition from the hexagonal to the orthorhombic phase, the prepared powder of sample 2 with hexagonal phase as the dominant phase was dispersed in distilled water and was then subjected to hydrothermal treatment in an autoclave at 200 °C for 24 h. The XRD pattern of the collected powder shown in Figure 5c indicates that the $CeOHCO_3$ phase is not stable at high temperatures and tends to be oxidized to a CeO_2 phase. In addition, the hexagonal phase vanished completely; however, a trace amount of orthorhombic phase was still detected (Figure 5c).

Time-dependent phase transition of $CeOHCO_3$: In order to understand the phase evolution process in the ethanol/water system, the reaction was prolonged for different periods of time, although the volume ratio of the solvent was kept constant. The experiments were carefully conducted in a solution system with different volume ratios of ethanol/water. Interestingly, the product obtained after 12 h was almost pure orthorhombic $CeOHCO_3$, as confirmed by the XRD pattern (Figure 6a). When the reaction time was prolonged to 20 h, hexagonal $CeOHCO_3$ appeared (Figure 6b). Furthermore, orthorhombic $CeOHCO_3$ almost disappeared and hexagonal $CeOHCO_3$ became the dominant phase when the reaction time was prolonged to 24 h (Figure 6c). As the reaction time increased, hexagonal $CeOHCO_3$ tended to transform back into the orthorhombic phase so that it became the dominant phase again (Figure 6d and e). This suggests

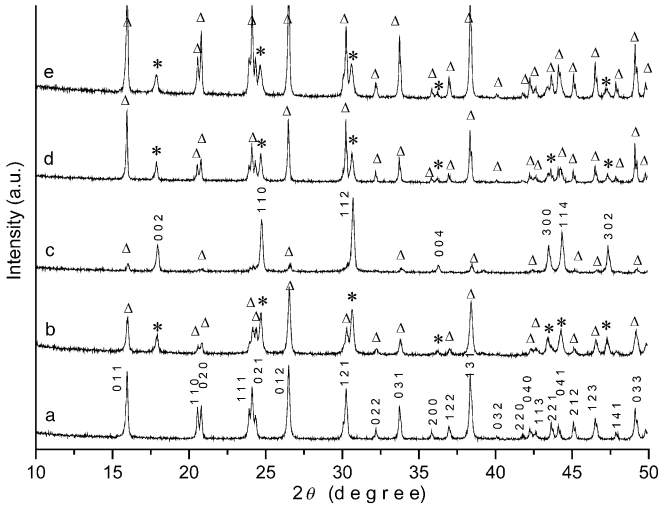

Figure 6. Influence of the reaction time on the phase transition in the presence of 5 mL ethanol + 15 mL distilled water. a) Pure orthorhombic $CeOHCO_3$, 12 h. b) A mixture of orthorhombic and hexagonal $CeOHCO_3$ (20 h). c) Almost pure hexagonal $CeOHCO_3$, 24 h. d) A mixture of orthorhombic and hexagonal $CeOHCO_3$ (36 h). e) A mixture of orthorhombic and hexagonal $CeOHCO_3$, 72 h. △ orthorhombic $CeOHCO_3$ (JCPDS file no. 41–13), ∗ hexagonal $CeOHCO_3$ (JCPDS file no. 32–189).

that there is a dynamic phase transition process between the orthorhombic and hexagonal phases in this reaction system.

The SEM images in Figure 7a and b show the coexistence of large orthorhombic crystals with rough surfaces and tiny hexagonal spheres with a size of 500 nm after reacting for 20 h. After the reaction was prolonged to 72 h, the smaller hexagonal spheres tended to vanish and orthorhombic crystals with smooth surfaces were observed (Figure 7c and d), resulting in the formation of a lot of prismatic crystals with smooth surfaces. The evident vanishing of the amount of hexagonal spheres suggests that there is a phase transformation from the metastable hexagonal phase to the orthorhombic phase in this system. In addition, Ostwald ripening can be expected to take place, because the spheres are much smaller than the orthorhombic crystals.

However, at the beginning of the reaction, the orthorhombic phase formed that gradually transformed into the hexagonal phase. This contradicts thermodynamic expectations so that a change in the experimental variables must exist that favors the formation of the metastable hexagonal phase from the stable orthorhombic one (Figure 6). According to Equation (4) above, hydroxy and carbonate ions are consumed upon formation of $CeOHCO_3$, so that the pH will become more acidic when the initial orthorhombic crystals

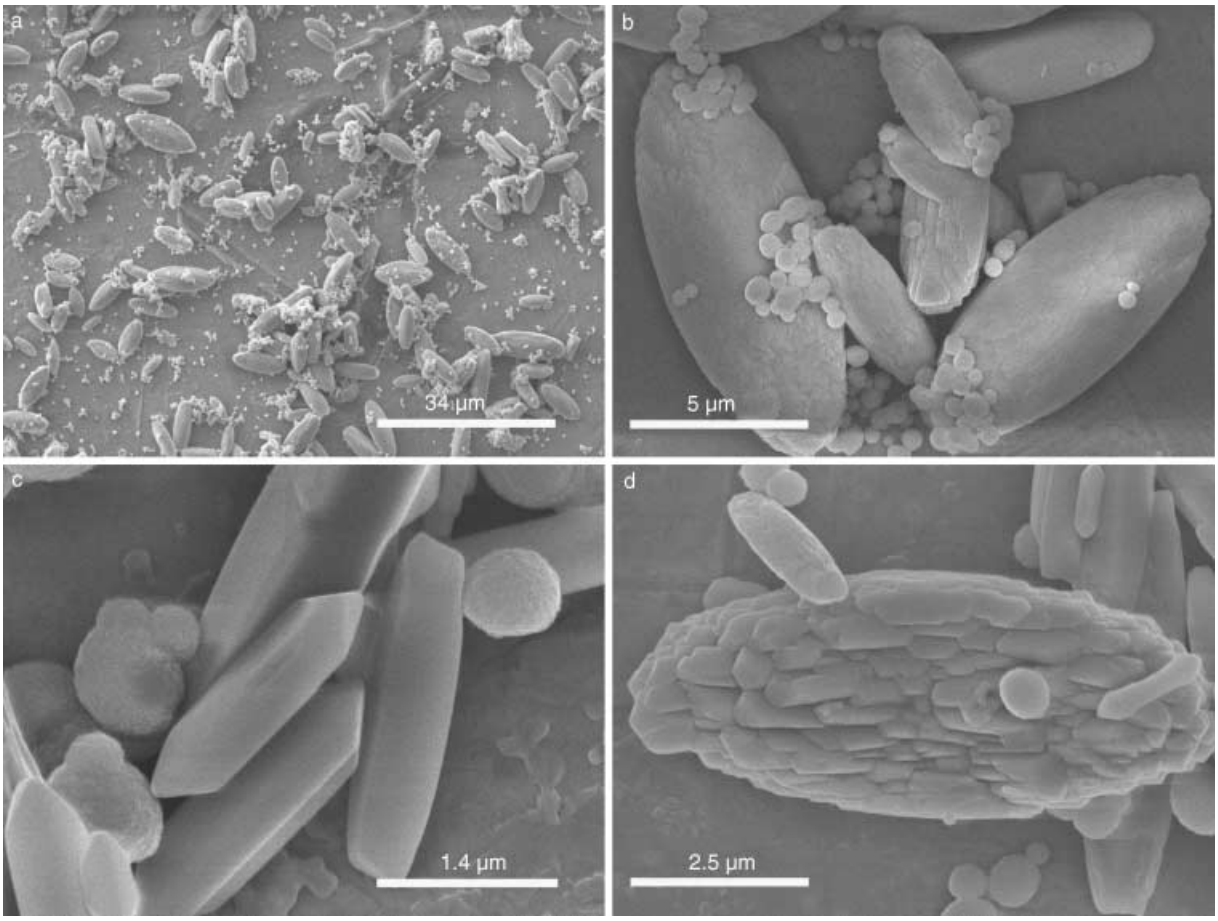

Figure 7. SEM images of samples obtained in presence of 5 mL ethanol + 15 mL water with different reaction times, at 80 °C. a) and b) Orthorhombic $CeOHCO_3$ was the dominant phase along with a little hexagonal $CeOHCO_3$ after reaction for 20 h. c) and d) Orthorhombic $CeOHCO_3$ was the dominant phase; hexagonal $CeOHCO_3$ spheres tended to disappear after a reaction time of 72 h, which indicated the transition process from hexagonal $CeOHCO_3$ to orthorhombic $CeOHCO_3$.

form. Because all hydroxides and carbonates are soluble in acid, this means an increased solubility, which could favor the formation of the kinetic hexagonal phase. When the solubility product of the more soluble hexagonal phase is reached, no more precipitation takes place so that the pH can be expected to stay constant and the thermodynamically driven transformation of the hexagonal into the orthorhombic phase can take place. It is interesting that the final, large, oval-like orthorhombic crystals are composed of crystallites with the equilibrium morphology of the orthorhombic structures, as shown in Figure 7d.

Variation of the ethanol/water ratio leads to similar phase-transformation phenomena. When the volume ratio of ethanol/water increases to 1:1, the product obtained after 1 day (Figure 8a) is composed of an almost identical amount of the two phases. However, when the reaction was prolonged to 2 days, the product was almost pure hexagonal phase (Figure 8b). After the reaction was prolonged to 3 days (Figure 8c), the intensity of the diffraction peaks from the orthorhombic phase increased, implying that the hexagonal phase transforms into the orthorhombic phase. The SEM image in Figure 9a clearly shows the coexistence of the large orthorhombic crystals and smaller spheres of the hexagonal phase. Because the difference in the size between hexagonal phase $CeOHCO_3$ and orthorhombic phase,

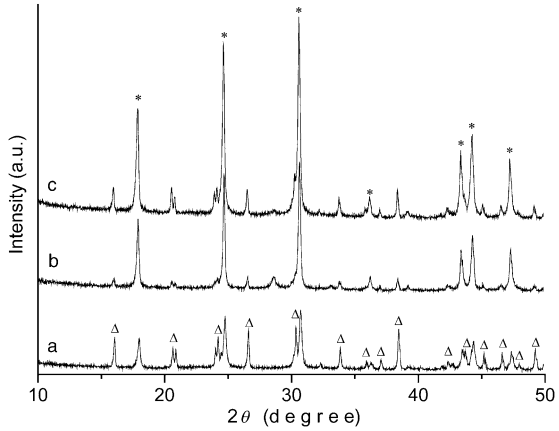

Figure 8. Influence of the reaction time on the phase transition in 10 mL ethanol + 10 mL distilled water at 80 °C: a) 1 day, b) 2 days, c) 3 days. * hexagonal $CeOHCO_3$, △ orthorhombic $CeOHCO_3$.

the smaller particles will have a greater solubility than the larger ones. According to the Ostwald ripening process, the smaller particles will dissolve and the large ones will grow further. The pure hexagonal phase is very difficult to capture because of this phase transformation. Thus, in this study, it was impossible to isolate the 100 % pure hexagonal

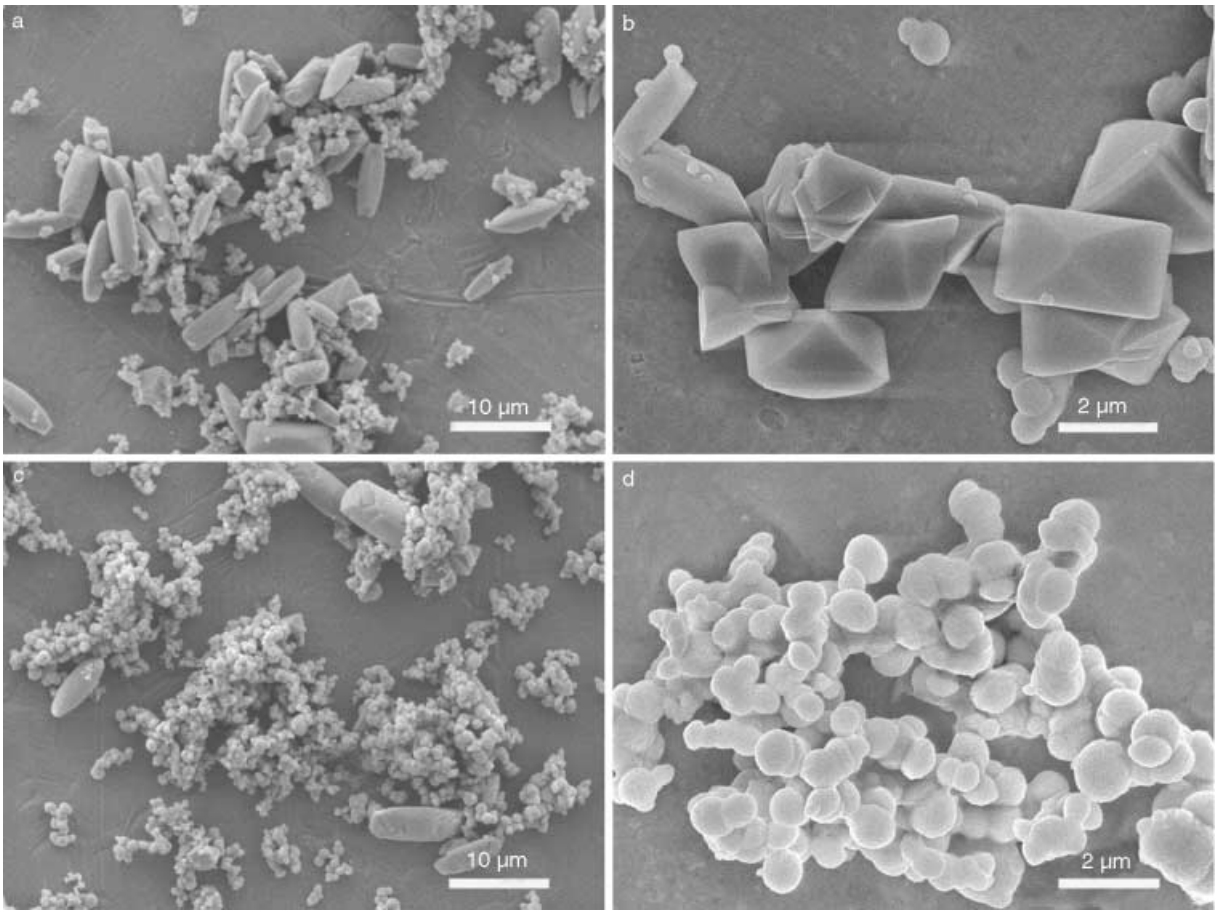

Figure 9. SEM images of samples at 80 °C, obtained in 10 mL ethanol + 10 mL water. a) A mixture with almost identical amounts of orthorhombic and hexagonal $CeOHCO_3$, 1 day (sample 3). b) High magnification image of some untransformed orthorhombic $CeOHCO_3$ particles as shown in a). c) and d) almost pure hexagonal $CeOHCO_3$, 2 days: c) a general view, d) high magnification image of hexagonal $CeOHCO_3$ crystals.

phase, and this further underlines that it is a metastable polymorph.

The XRD pattern in Figure 1c shows that the relative intensity of the 110, 012, and 121 diffraction peaks is much enhanced, whereas the 020 and 200 peaks are weakened compared to those shown in Figure 1a. The enlarged SEM image in Figure 9b shows that the orthorhombic crystals tend to become short quasioctahedron-like crystals with well-developed exposed (012) and (121) faces. For orthorhombic $CeOHCO_3$, the angle (Φ) between the (012) face and the (121) face was calculated to be $\Phi \approx 130^{o}$ with Equation (6).

$$\cos\phi = \frac{\frac{h_1h_2}{a^2} + \frac{k_1k_2}{b^2} + \frac{l_1l_2}{c^2}}{\sqrt{\left(\frac{h_1^2}{a^2} + \frac{k_1^2}{b^2} + \frac{l_1^2}{c^2}\right)\left(\frac{h_2^2}{a^2} + \frac{k_2^2}{b^2} + \frac{l_2^2}{c^2}\right)}} \quad (6)$$

This value fits quite well with that of the crystals measured from Figures 4 and 9b. The short aspect ratio (as shown in Figures 4 and 9b) and smooth surface structure in the 1:1 (volume ratio, 1:1, v/v) ethanol/water solution is totally different from the rough surface with caves obtained in ethanol-rich solutions, such as 1:3 ethanol/water (v/v).

As discussed above, the product obtained after 2 days under the conditions of Figure 8 was found to be almost pure hexagonal phase. Only minor amounts of the orthorhombic phase can be detected by the XRD (Figure 8b). In fact, the SEM image in Figure 9c clearly shows that the majority of particles are spheres with an average size of $\approx$500–800 nm (see also enlarged SEM image in Figure 9d). These results also suggest that the phase equilibrium between these two phases responds to a change in the experimental parameters, such as pH, as is expected from Equation (4).

As the duration of the experiment increased, the amount of the metastable hexagonal phase decreased and the amount of orthorhombic phase increased again, according to thermodynamic expectations. This result suggested that the trapping of the pure hexagonal phase is difficult but possible. More detailed work needs to be carried out in the future.

Optical properties of cerium compounds: The optical properties of rare-earth hydroxycarbonates have rarely been investigated until now. Room-temperature luminescence spectra of the samples with different compositions and phases were investigated in detail (Figure 10). A strong ultraviolet emission band centered at $\lambda = 332$ nm for the pure orthorhombic $CeOHCO_3$ (Figure 10a) was observed for the first time, to the best of our knowledge. A relatively weak emission band centered at 396 nm (Figure 10a) is also observed. It has the same position as that of the almost pure hexagonal $CeOHCO_3$ (Figure 10d), which is consistent previous reports.[24] The presence of an emission at 396 nm in sample 1 could be attributed to a minor amount of poorly crystallized hexagonal $CeOHCO_3$ phase, which can not be detected by the XRD (see Figure 1a), but which can be detected in the SEM image (see smaller spheres in Figure 2a). The samples with a mixture of orthorhombic and hexagonal phases (Figure 10b and c) display a strong peak centered at 342 nm,

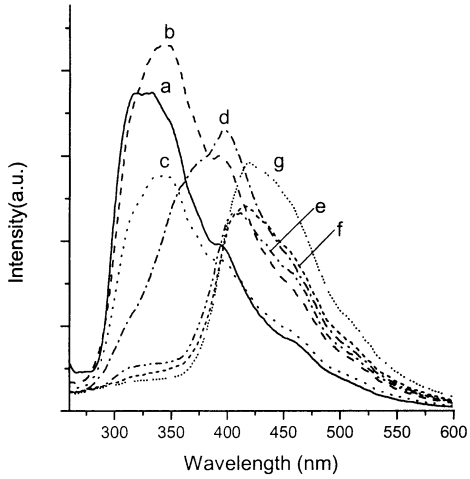

Figure 10. Photoluminescence spectra of cerium compounds synthesized at 80 °C. a) Pure orthorhombic $CeOHCO_3$ (sample 1, pure water, 1 day). b) A mixture of almost pure hexagonal and some orthorhombic $CeOHCO_3$ (sample 2, $R = 3$, 1 day). c) A mixture of almost two nearly identical amounts of orthorhombic and hexagonal $CeOHCO_3$ (sample 3, $R = 1$, 1 day). d) Almost pure hexagonal $CeOHCO_3$ ($R = 1$, 2 days). e) A mixture of cubic CeO_2, and well as hexagonal and orthorhombic $CeOHCO_3$ (sample 4, $R = 1/3$, 1 day). f) A mixture of almost pure cubic CeO_2 and orthorhombic $CeOHCO_3$ (sample 5, $R = 3/17$, 1 day). g) A mixture of almost pure cubic CeO_2 and traces of orthorhombic $CeOHCO_3$ (sample 6, $R = 1/9$, 1 day). Solvent composition: total volume = 20 mL, R = volume of distilled water:volume of anhydrous alcohol (v/v), excitation wavelength = 230 nm.

which has an evident red shift relative to that observed in Figure 10a (sample 1). This slight red shift of 10 nm could be caused by overlap of the emission bands for orthorhombic and hexagonal $CeOHCO_3$ (Figure 10b and c).

When the product contains the CeO_2 phase, the emission was found to be dominated by the characteristic emission of the CeO_2 nanoparticles. The main emission peak for the samples containing cubic CeO_2, as well as hexagonal and orthorhombic $CeOHCO_3$ (sample 4), and a mixture containing a majority of cubic CeO_2 nanocrystals and a small amount of the orthorhombic $CeOHCO_3$, is located at 406 and 416 nm, respectively (Figure 10e and f). However, a weak shoulder at $\lambda \approx 330$ nm still indicates the presence of the orthorhombic phase. Figure 10g shows a strong luminescence band at 420 nm for pure CeO_2 nanocrystals. Again, the trace of the orthorhombic phase could be detected as a small shoulder at $\approx$330 nm. The slight emission shift of the strong bands was caused by the overlapping effect of the different phases existing in the products. The results show that either the UV emission intensity or the emission position could be adjusted by controlling the relative phase content in the product.

Conclusions

In summary, we demonstrated for the first time that a mild solution method can be adopted for the selective synthesis of orthorhombic and metastable hexagonal $CeOHCO_3$, and cubic CeO_2 nanocrystals in an ethanol/water solution.

The competitive reactions in the ethanol/water system, the phase formation, and the shape evolution were fully investigated. They were found to be strongly dependent on the composition of the reaction media. Addition of ethanol to water has a significant influence on the formation and transition of different phases. The influence of the ethanol content in the mixed solvent and the reaction time on the phase formation and shape of orthorhombic and hexagonal $CeOHCO_3$ crystals was discussed in detail. The results show that the metastable hexagonal $CeOHCO_3$ can be temporarily trapped in a large excess under very mild conditions (80°C) in an ethanol/water mixture; however, it transforms into the more stable orthorhombic phase over time, in agreement with thermodynamic expectations. In addition, the reverse event was also detected. Here, the transition of the orthorhombic phase into the metastable hexagonal phase was observed as a probable result of initial pH changes on the precipitation of $CeOHCO_3$, so that here, the kinetic pathway was dominant.

The optical properties of the products with different phases and compositions were investigated and revealed that the UV emission intensity or the emission position could be tuned by controlling the relative phase content in the product.

This study added a new example for selectively controlling different cerium compounds by manipulating the balance between kinetics and thermodynamics in a simple mixed solvent system at moderate temperatures. It has to be pointed out that the reported approach can potentially be up-scaled so that this study is a promising approach for the defined generation of different cerium compounds with respect to shape and optical characteristics. The reported ethanol/water system may also represent a promising medium for the selective synthesis of other inorganic materials with different phases and polymorphs.

Acknowledgement

S.-H.Y. acknowledges the special funding support from the Centurial Program of the Chinese Academy of Sciences, the Distinguished Youth Fund, the Distinguished Team (NSFC, No. 20325104, 20321101), and NSFC No. 50372065 of the National Science Foundation of China for financial support. H.C. thanks the Max Planck Society for funding support.

[1] T. Justel, H. Nikol, C. Ronda, *Angew. Chem.* **1998**, *110*, 3250; *Angew. Chem. Int. Ed.* **1998**, *37*, 3084.
[2] G. Y. Adachi, N. Imanaka, *Chem. Rev.* **1998**, *98*, 1479.
[3] M. S. Palmer, M. Nearock, M. M. Olken, *J. Am. Chem. Soc.* **2002**, *124*, 8452.
[4] J. W. Stouwdam, F. C. J. M. van Veggel, *Nano Lett.* **2002**, *2*, 733.
[5] Y. Hasegawa, S. Thongchant, Y. J. Wada, H. Tanka, K. Tomoji, S. Takao, H. Mori, S. Yanagida, *Angew. Chem.* **2002**, *114*, 2177; *Angew. Chem. Int. Ed.* **2002**, *41*, 2073.
[6] Y. P. Fang, A. W. Xu, R. Q. Song, H. X. Zhang, L. P. You, J. C. Yu, H. Q. Liu, *J. Am. Chem. Soc.* **2003**, *125*, 16025.
[7] X. Wang, Y. D. Li, *Angew. Chem.* **2002**, *114*, 4984; *Angew. Chem. Int. Ed.* **2002**, *41*, 4790.
[8] S. Velu, K. Suzuki, *Top Catal.* **2003**, *22*, 235.
[9] W. Van Kooten, C. M. K. J. Van den Bleek, *Catal. Lett.* **1999**, *63*, 227.
[10] Q. Fu, H. Saltsburg, M. Flytzani-Stephanopoulos, *Science* **2003**, *301*, 935.
[11] K. Tanaka, Y. Inoue, S. Okamoto, *Jpn. J. Appl. Phys. Part 1* **1997**, *36*, 3517.
[12] E. Danielson, M. Devenney, D. M. Giaquinta, J. H. Golden, R. C. Haushalter, E. W. Mcfarland, D. M. Poojary, C. M. Reaves, W. H. Weinberg, X. D. Wu, *Science* **1998**, *279*, 831.
[13] H. J. Kang, P. Dai, J. W. Lynn, M. Matsuura, J. R. Thompson, S. C. Zhang, D. N. Argyriou, Y. Onose, Y. Tokura, *Nature* **2003**, *423*, 522.
[14] T. Sato, T. Kamiyama, T. Takahashi, K. Kurahashi, K. Yamada, *Science* **2001**, *291*, 1517.
[15] Y. Aoki. , H. Sato, Y. Komaba, *Phys. Rev. B* **1996**, *54*, 12172.
[16] M. Jaime, R. Movshovich, G. R. Stewart, W. P. Beyermann, M. G. Berisso, M. F. Hundley, P. C. Canfield, J. Sarrao, *Nature* **2000**, *405*, 160.
[17] V. Keppens, D. Mandrus, B. C. Sales, B. C. Chakoumakos, P. Dai, R. Coldea, M. B. Maple, D. A. Gajewski, E. J. Freeman, *Nature* **1998**, *395*, 876.
[18] Z. H. Han, Y. T. Qian, J. Yang, G. Q. Lu, *J. Mater. Chem.* **2003**, *13*, 150.
[19] W. P. Hsu, L. Ronnquist, E. Matijevic, *Langmuir* **1988**, *4*, 31.
[20] H. C. Wang, C. H. Lu, *Mater. Res. Bull.* **2002**, *37*, 783.
[21] G. S. Li, S. H. Feng, L. P. Li, *J. Solid State Chem.* **1996**, *126*, 74.
[22] C. H. Lu, H. C. Wang, *Mater. Sci. Eng. B* **2002**, *B90* , 138.
[23] Q. Li, Z. H. Han, M. W. Shao, X. M. Liu, Y. T. Qian, *J. Phys. Chem. Solids* **2003**, *64*, 295.
[24] Z. H. Han, N. Guo, K. B. Tang, S. H. Yu, H. Q. Zhao, Y. T. Qian, *J. Cryst. Growth* **2000**, *219*, 315.
[25] See a review and references therein, H. Cölfen, S. Mann, *Angew. Chem.* **2003**, *115*, 2452; *Angew. Chem. Int. Ed.* **2003**, *42*, 2350.
[26] S. R. Dickinson, K. M. McGrath, *J. Mater. Chem.* **2003**, *13*, 928.
[27] a) G. Falini, S. Fermani, M. Gazzano, A. Ripamonti, *Chem. Eur. J.* **1997**, *3*, 1807b) G. Falini, S. Fermani, M. Gazzano, A. Ripamonti, *J. Chem. Soc. Dalton Trans.* **2000**, 3983.
[28] a) See a review and references therein: S. H. Yu, *J. Ceram. Soc. Jpn.* **2001**, *109*, S65; b) S. H. Yu, J. Yang, Z. H. Han, Y. Zhou, R. Y. Yang, Y. Xie, Y. T. Qian, Y. H. Zhang, *J. Mater. Chem.* **1999**, *9*, 1283; c) S. H. Yu, L. Shu, J. Yang, Z. H. Han, Y. T. Qian, Y. H. Zhang, *J. Mater. Res.* **1999**, *14*, 4157.
[29] M. Haase, A. P. Alivisatos, *J. Phys. Chem.* **1992**, *96*, 6756; b) S. H. Tolbert, A. P. Alivisatos, *Science* **1994**, *265*, 373.
[30] K. Murakoshi, H. Hosokawa, N. Tanaka, M. Saito, Y. Wada, T. Sakata, H. Mori, S. Yanagida, *Chem. Commun.* **1998**, 321.
[31] G. Falini, M. Gazzano, A. Ripamonti, *Chem. Commun.* **1996**, 1037.
[32] J. Lahiri, G. Xu, D. M. Dabbs, N. Yao, I. A. Aksay, J. T. Groves, *J. Am. Chem. Soc.* **1997**, *119*, 5449.
[33] F. Manoli, E. Dalas, *J. Cryst. Growth* **2000**, *218*, 359.
[34] L. M. Qi, J. Li, J. M. Ma, *Chem. J. Chin. Univ.* **2002**, *23*, 1595.
[35] D. B. Yu, S. H. Yu, S. Y. Zhang, J. Zuo, D. B. Wang, Y. T. Qian, *Adv. Funct. Mater.* **2003**, *13*, 497.
[36] W. S. Sheldrick, M. Wachhold, *Angew. Chem.* **1997**, *109*, 214; *Angew. Chem. Int. Ed. Engl.* **1997**, *36*, 206.
[37] C. Y. Tai, F. B. Chen, *AIChE J.* **1998**, *44*, 1790.
[38] S. H. Yu, H. Cölfen, M. Antonietti, *J. Phys. Chem. B* **2003**, *107*, 7396.
[39] M. Hirano, E. Kato, *J. Am. Ceram. Soc.* **1996**, *79*, 777.

Received: December 25, 2003
Published online: April 28, 2004

